Gasification Pathways and Reaction Mechanisms of Primary Alcohols in Supercritical Water

Brian R. Pinkard[a]*, *John C. Kramlich*[a], *and Igor V. Novosselov*[a,b]

[a] University of Washington, Mechanical Engineering Department, 3900 E Stevens Way, Seattle, WA 98195

[b] University of Washington, Institute for Nanoengineered Systems, Seattle, WA 98195

* Corresponding Author: pinkardb@uw.edu, +1 253 3105882

ORCID 0000-0002-4517-4712

ABSTRACT

Supercritical water gasification is a promising waste-to-energy technology with the ability to convert aqueous and/or heterogeneous organic feedstocks to high-value gaseous products. Reaction behavior of complex molecules in supercritical water can be inferred through the reaction pathways of model compounds in supercritical water. Methanol, ethanol, and isopropyl alcohol are gasified in a continuous supercritical water reactor at temperatures between 500 and 560 °C, and for residence times between 3 and 8 s. *In situ* Raman spectroscopy is used to rapidly identify and quantify reaction products. The results suggest the dominance of chain-branching, free radical reaction mechanisms that are responsible for decomposing primary alcohols in the supercritical water environment. The presence of a catalytic surface is proposed to be highly significant for initiating radical reactions. Global reaction pathways are proposed, and mechanisms for free radical reaction initiation, propagation, and termination are discussed in light of these and previously published experimental results.

Keywords: Supercritical, Gasification, Reaction Mechanisms, Free Radical, Alcohol

1. Introduction

Greenhouse gas emissions from the combustion of fossil fuels have stimulated governments and industry to explore alternative methods for valorizing energy from renewable sources. Supercritical water (SCW) continues to gain relevance as a green reaction medium for gasification and/or oxidation of organic compounds. As water is heated and pressurized past its critical point (374 °C, 22.1 MPa), the H-bond network begins to break apart and the dielectric constant decreases, resulting in high solubility of simple and complex organic molecules in SCW [1]. High temperatures accelerate the breakdown of most organic molecules, either via endothermic gasification pathways, which yield H_2, CO, CO_2, and CH_4 or via exothermic oxidation pathways that yield H_2O and CO_2 [2]. Near the critical point, high quantities of H^+ and OH^- ions create an environment favorable for ionic chemistry pathways. At temperatures well above the critical point, the low-density of SCW is an ideal medium for rapid pyrolysis, hydrolysis, and free-radical reaction mechanisms [3]. SCW has been studied as a viable reaction medium to produce gaseous fuel from biomass, sewage sludge, plastics, and agricultural residues [1-4].

The gaseous product from SCWG (syngas) is rich in H_2 with varied yields of CO and CH_4. This syngas can be used for production of liquid fuels via Fischer-Tropsch processes, or hydrogen can be purified and used in industrial processes for hydrocracking, hydrotreating or ammonia production [5, 6]. Key reactions determining the final gaseous yields are the water-gas shift (WGS) reaction:

$$CO + H_2O \leftrightarrow CO_2 + H_2$$

and methanation reactions:

$$CO + 3H_2 \leftrightarrow CH_4 + H_2O$$

$$CO_2 + 4H_2 \leftrightarrow CH_4 + 2H_2O$$

Methanation reactions are exothermic, thus higher temperatures minimize methane production.

Many technical barriers still hinder industrial-scale SCWG. For example, salts in heterogeneous feedstocks precipitate in SCW and corrode or foul reactor components. Char formation is also common, especially when high concentrations of aromatic compounds are present. Workarounds are available for the

fouling and clogging problems, however the materials, designs, and processing regimes required tend to be too costly to implement at the industrial scale. For example, char formation can be avoided by running at low feedstock concentrations (e.g. 1 wt%), but such a processing regime is too energetically costly to be feasible.

Among the many challenges hindering successful implementation of SCWG at the industrial scale is a better understanding of chemical reactions for accurate process simulation and modeling Accurate knowledge of reaction mechanisms and physical transport properties of common molecules present during SCWG allow more novel methods for controlling char formation and reactor fouling to be conceptualized, modeled, designed, and implemented. Basic knowledge of these fundamental phenomena is an important step towards designing robust SCWG reactors for industrial-scale waste treatment and hydrogen production.

1.1. Batch vs. Continuous Reactors

The study of reaction chemistry in continuous supercritical water reactors (SCWRs) is of particular interest. Many past studies of model alcohol decomposition in SCW have been conducted in non-reactive, quartz batch reactors [7, 8]. While experiments in batch reactors yield important scientific insights, batch reactors have different catalytic and mass transfer behavior than continuous reactors [8, 9]. Continuous operation is preferred for an industrial-scale system in order to maximize process throughput and yields. Briefly, most continuous reactors are constructed from nickel-base alloys, which are catalytic to gasification reactions. Flow-through operation in tubular reactors increases the interaction of reactants with catalytic reactor walls, especially when the flow regime is turbulent. Finally, reactants in a batch system typically require >60 s to reach reaction temperatures, which creates challenges in interpreting chemical reaction behavior, while continuous reactors can facilitate near-instantaneous reagent heating to reaction temperatures.

Studies of reaction chemistry in continuous reactors allows for (i) simulating reaction behavior in practical systems, (ii) *in situ* data collection for rapidly conducting experiments at short or long residence

times [10], and (iii) near-instantaneous reactant heating and mixing using post-critical injection to achieve a clear reaction starting point [11]. However, it must be noted that inert wall batch reactors offer an opportunity to characterize SCWG chemistry in the absence of a catalytic surface; these are useful benchmarks for understanding the influence of catalysis on the reactions.

1.2. SCWG of Model Alcohols

According to Chakinala et al. [12], ethanol and methanol are stable in SCW at temperatures up to 600 °C in the absence of a catalyst. This claim suggests that thermal, unimolecular decomposition of primary alcohols is unlikely in SCW at temperatures below 600 °C. In a study using a batch autoclave reactor, ethanol is reported to produce the highest yield of gaseous products among all alcohols, followed by methanol. All higher chain alcohols were reported to yield lower quantities of gas due to the formation of refractory liquid products. Broadly, all previous studies of primary alcohol gasification in SCW have found that higher temperatures and longer residence times increase conversion to gaseous products, while variations in pressure produce no measurable effect.

1.2.1. Methanol Gasification

Several studies have investigated methanol decomposition in SCW. Boukis et al. [13] reformed methanol in an Inconel 625 continuous, tubular SCWR at 400 to 600 °C, residence times from 3 to 100 s, and initial methanol loadings from 5 to 64 wt%. H_2, CO, CO_2, and trace amount of CH_4 were detected in the gaseous product. Bennekom et al. [14] gasified methanol in a continuous reactor at temperatures between 450 and 650 °C for residence times between 6 and 173 s. Yields of H_2, CO, and CO_2 were observed. Trace CH_4 yields were reported. Analysis of liquid products revealed trace yields of formaldehyde and formic acid. It was hypothesized that both existed as short-lived reaction intermediates, which is consistent with previous research demonstrating formic acid as an intermediate of the WGS reaction [10, 15].

DiLeo and Savage [7] investigated the role of nickel as a catalyst for methanol gasification in SCW. The presence of a nickel wire in a quartz batch reactor increased conversion from 20% after 2 h to 90%

after 5 min at 550 °C. It should be noted that nickel catalysis in a continuous reactor is even more significant, as the catalytic effect in the batch setup is limited by the diffusion rate of methanol molecules. H_2, CO, and CO_2 were the only products consistently detected in the gaseous phase.

Chakinala et al. [12] proposed that methanol can decompose to gaseous products in SCW primarily through C-H bond scission to a hydroxymethyl radical (CH_2OH) or O-H bond scission to a methoxy radical (CH_3O) followed by loss of an additional H to reach formaldehyde (CH_2O). Formaldehyde was proposed to decompose to CO and H_2 or to reach formic acid (HCOOH) via oxidation with an OH radical. A minor pathway to methane via the formation of a methyl (CH_3) radical by C-O bond scission is also proposed.

1.2.2 Ethanol Gasification

Schanzenbächer et al. [16] gasified ethanol in a continuous SCWR at temperatures from 433 to 494 °C, constant pressure of 24.6 MPa, and residence times from 2 to 12 s. Maximum conversion was reported as 16.5%; only acetaldehyde (C_2H_5O) was identified as a reaction product.

Arita et al. [17] studied non-catalytic reaction pathways of ethanol in a batch SCWR. Temperatures from 450 to 500 °C were maintained for 10 to 60 minutes, with primary reaction products identified as H_2, CH_4, and CO_2, and minor yields of CO, acetaldehyde, ethylene, and ethane. Two competing reaction pathways were proposed: (i) dehydrogenation of ethanol to acetaldehyde followed by acetaldehyde decomposition to CO and CH_4, or (ii) dehydration of ethanol to ethylene followed by hydrogenation of ethylene to ethane. Global reactions for the two pathways are as follows:

$$C_2H_5OH \rightarrow C_2H_4O + H_2$$

$$C_2H_4O \rightarrow CH_4 + CO$$

$$CO + H_2O \rightarrow CO_2 + H_2$$

$$C_2H_5OH \rightarrow C_2H_4 + H_2O$$

$$C_2H_4 + H_2 \rightarrow C_2H_6$$

Chakinala et al. [12] hypothesized ethanol decomposition pathways via batch reactor studies. Like methanol, O-H or C-H bond scission is theorized as the dominant mechanism to produce acetaldehyde. At

various points in the proposed reaction network, the C-C bond can be broken, forming a methyl radical, which ultimately forms CH_4. The proposed network is based on observed yields of H_2, CO, CO_2, CH_4, and ethane.

1.2.3. Isopropyl Alcohol Gasification

Previous work on SCWG of 1- or 2-propanol is limited. Antal Jr., Carlsson, and Xu [18] report yields of propene (C3H6) and 1-propanol after acid-catalyzed dehydration of 2-propanol in subcritical water at 34.5 MPa and 320 °C for residence times up to 100 s. Chakinala et al. [12] gasified 1-propanol in SCW, noting trace yields of benzene and toluene. The postulated reaction network again includes initial C-H and O-H bond scission steps, leading to acetone (C_3H_6O), which is thought to break down to CH_4 and CO. Other theorized steps include reactions to form ethylene, ethane, and various intermediate products.

1.3. Reaction Mechanisms and Pathways

The experiments conducted in this study are meant to fully elucidate the dominant reaction mechanisms involved in primary alcohol decomposition in SCW. While previous studies have roughly defined the reaction networks, many discrepancies exist, and the conditions necessary for full conversion of alcohols in a continuous reactor are still largely unknown. For practical relevance, a continuous reactor is used, and *in situ* Raman spectroscopy allows for collected product yield data after reactions at short residence times.

2. Material and Methods

A continuous, tubular SCWG reactor is used to perform all experiments, manufactured from Inconel 625 with a surface-to-volume ratio (S/V) of 13.1 cm^{-1}. Pure methanol, ethanol, or IPA were continuously introduced into the SCWG reactor at an overall volumetric loading of 10 vol%, corresponding to 8.09 wt%, 8.06 wt%, and 8.03 wt% initial respective mass fractions. All reagents were used as received without further purification. The reactor components and design methodology have been described

thoroughly elsewhere [9, 10]. Briefly, a custom mixing section is used to inject cold reagent into a bulk flow of supercritical deionized water, as shown in Figure 1. A 1:9 volumetric flow ratio of reagent:water is selected to achieve rapid mixing and heating as detailed in Tiwari et al. [11]. Post-critical injection achieves a well-defined reaction initiation point, and a heat exchanger rapidly quenches products after a pre-defined residence time. All reactants and products exist in a well-mixed, supercritical fluid phase at reaction conditions.

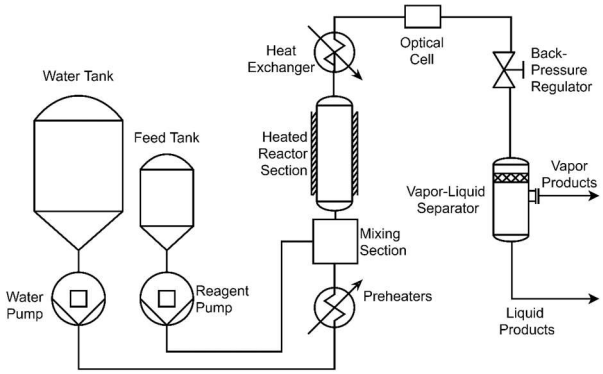

Figure 1: Schematic of continuous SCWG reactor used to conduct all experiments

Raman spectra are collected *in situ* for each experimental condition, using a flow-through optical cell and a fiber-optic immersion Raman probe operating in the backscatter configuration [19]. Spectra are translated both to qualitative (product identification) and quantitative (molecular concentrations) data relevant to understanding reaction pathways and rates. Indirect hard modeling (IHM) is used for accurate quantitative Raman spectroscopy for calculating product yields [20, 21]. PEAXACT spectral processing software is used to perform IHM. Quantitative calibration of Raman spectra was achieved via an indirect methodology closely aligned with that described by Beumers et al. [22] where an elemental balance of reactor inputs and outputs is used to achieve calibration.

Experimental temperature was varied from 500 to 560 °C, with residence times from 3 to 8 s for each alcohol at each temperature. Residence times were varied by changing the flow rates of water and reagent, using the density of water at reaction conditions and the known internal volume of the reactor to calculate necessary mass flow rates for a given residence time. Real-time variations in the Raman spectra were used to determine when the reactor had reached steady state between each experimental condition.

Due to the inherent challenge of repeatedly performing SCWG experiments, replicate experiments were not performed. Instead, five replicate Raman spectra were captured for each experimental condition, thus the error measurements presented on all figures represent an overall error in data collection and processing, not experimental error. Gasification efficiency, the ratio of the mass fraction of the gaseous products to the mass fraction of the reagent, is used as a key metric to quantify the efficacy of the SCWG process at each tested condition.

3. Results

3.1. Methanol

SCWG of methanol primarily yields H_2 and CO, with secondary yields of CO_2 and trace formaldehyde production, as shown in Figure 2. These profiles illustrate the sequential nature of product formation; H_2 is detectable at 4 s, followed by CO at 5 s, and CO_2 at 7 s. Formaldehyde is confirmed as a short-lived reaction intermediate; however, no yields of formic acid or methane are detected. We propose the global reaction network in Figure 3, with methanol dehydrogenating to formaldehyde, followed by decomposition to CO and H_2, and lastly the WGS to convert CO to CO_2.

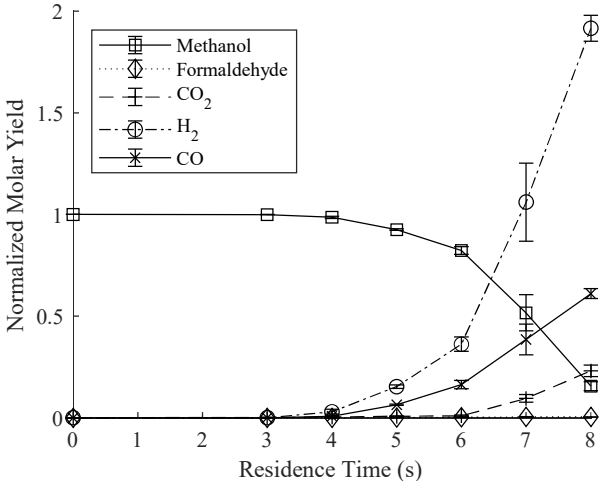

Figure 2: Formation and decomposition of reaction products during SCWG of methanol at 560 °C

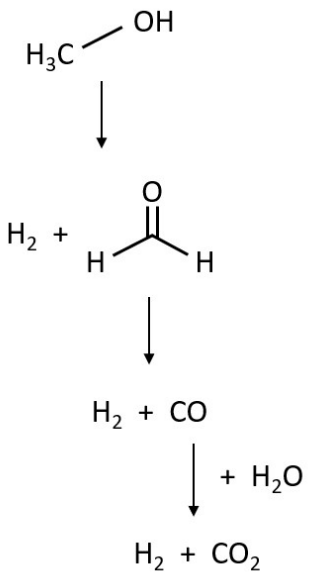

Figure 3: Methanol decomposition network in supercritical water

Our results indicate that the reaction mechanisms hypothesized by Chakinala et al. [12] to generate formic acid (formaldehyde oxidation) or methane (methyl radical generation) are unlikely to be active during SCWG. Trace methane yields have been reported [13, 14], but it is more likely that secondary methanation reactions are responsible for this observation. The time scales and temperatures necessary for methanol conversion in these experiments are similar to those reported for continuous SCWG of methanol by Boukis et al. [13] and Bennekom et al. [14]. Conversion rates at similar conditions were much slower in quartz batch reactors as reported by DiLeo and Savage [7], highlighting the significance of the catalytic reactor walls.

The WGS reaction is responsible for the observed maximum CO_2 yield of 0.23 mol-CO_2/mol-MeOH, but low yields indicate that the WGS reaction does not have sufficient residence time to reach completion. Full conversion of methanol along the network in Figure 3 would result in a maximum of 1 mol-CO_2/mol-MeOH and 3 mol-H_2/mol-MeOH. Full conversion of CO would increase H_2 yields past the observed maximum of 1.92 mol-H_2/mol-MeOH. Gasification efficiency (GE) is plotted against residence time for all tested temperatures in Figure 4. GE approaches values above 100% at 560 °C, due to the conversion of liquid H_2O to gaseous H_2 via the WGS. No other methanol decomposition products are

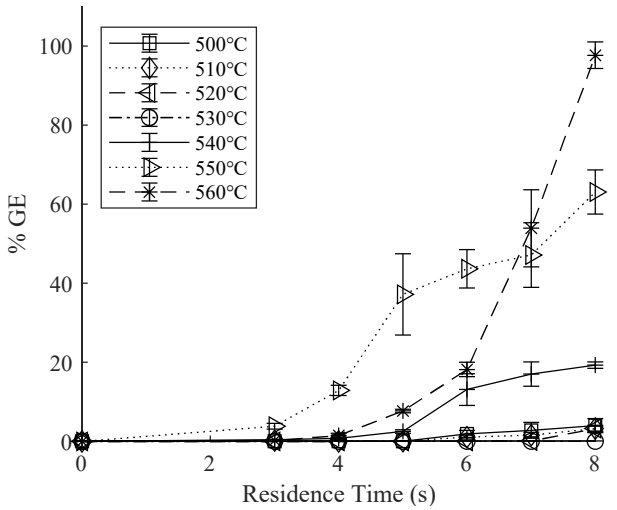

Figure 4: Gasification Efficiency of methanol at all tested temperatures

detected over the tested temperature and residence time range, and reaction profiles at all temperatures follow similar trends. Plots of compound formation and decomposition at all tested temperatures are available in Figure S1, and a representative Raman spectrum of methanol gasification products is shown in Figure S5.

3.2. Ethanol

Acetaldehyde and ethylene are the first observable products during the SCWG of ethanol at 560 °C, as shown at 3 s in Figure 6. This is followed by a significant increase in H_2, CO, and CH_4 yields at 5 s, as seen in Figure 5. Acetaldehyde yields continue to increase to a maximum of 0.12 mol-C_2H_4O/mol-EtOH at 6 s, followed by a similarly paced decrease to 0.005 mol-C_2H_4O/mol-EtOH, confirming its role as a short-lived intermediate. Once sufficient H_2 is generated for ethylene hydrogenation, ethane emerges as a detectable product at 6 s. Finally, a CO_2 yield of 0.04 mol-CO_2/mol-EtOH is measured at 8 s, again resulting from the WGS reaction. Figure 5 demonstrates that H_2, CO, and CH_4 are produced in nearly equimolar quantities, reaching maximum respective yields of 0.85 mol-H_2/mol-EtOH, 0.84 mol-CO/mol-EtOH and 0.91 mol-CH_4/mol-EtOH. This supports the hypothesis that acetaldehyde decomposition is responsible for

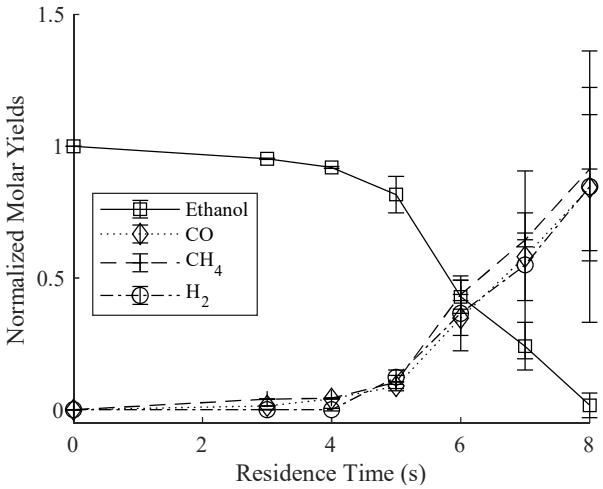

Figure 5: Formation and decomposition of major reaction products during SCWG of ethanol at 560 °C

the formation of CO and CH_4, with molar CO yields slightly lower due to consumption via the WGS. The trends described here are also observed during SCWG of ethanol at other tested temperatures; these formation and decomposition profiles are available in Figures S2 and S3.

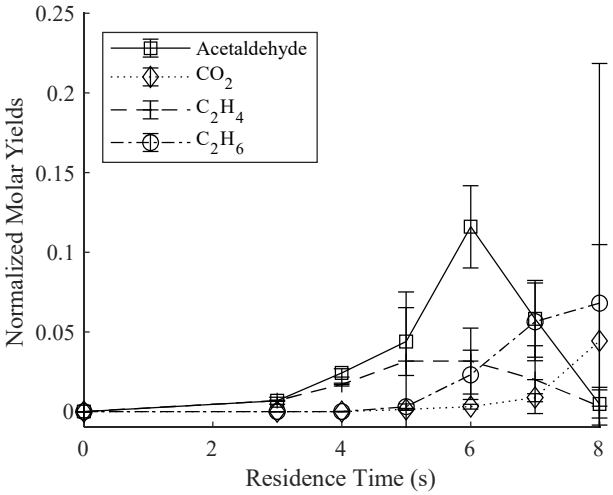

Figure 6: Formation and Decomposition of minor reaction products during SCWG of ethanol at 560 °C

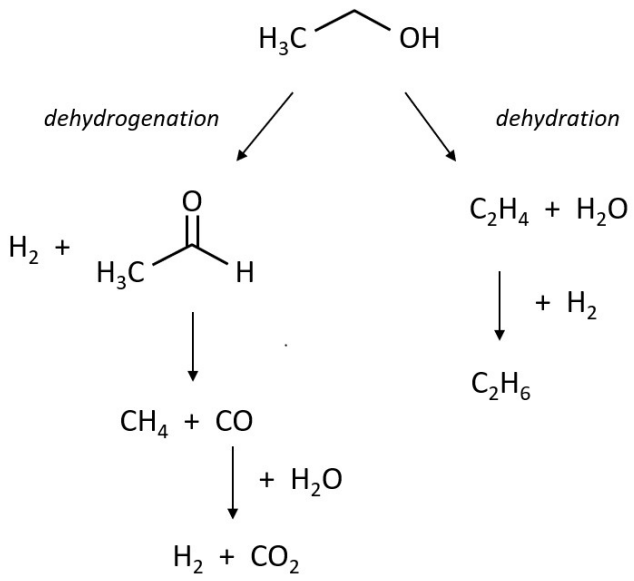

Figure 7: Ethanol decomposition network in supercritical water

Interpreting the observed product yields, ethanol decomposition follows the reaction pathways illustrated in Figure 7, confirming the global reactions proposed by Arita et al. [17]. However, the time scale for conversion at similar temperatures is orders of magnitude quicker during continuous gasification, again attributable to the catalytic wall effect. Two competing reaction pathways are active, the primary being dehydrogenation to acetaldehyde, with a secondary pathway of dehydration to ethylene. Acetaldehyde is rapidly converted to CO and CH_4, while ethylene can hydrogenate to ethane if suitable H_2 is present. The production of ethane through the reaction of two methyl radicals does not appear to be an active pathway,

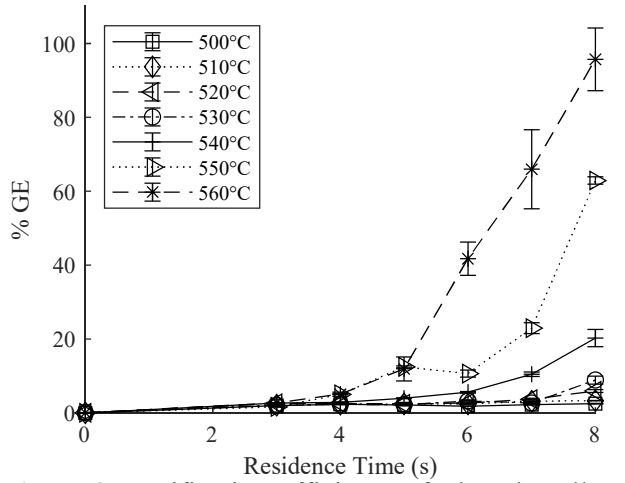

Figure 8: Gasification Efficiency of ethanol at all tested temperatures

considering that ethane is only produced subsequent to ethylene production. This also appears to indicate that ethane dehydrogenation to ethylene is a negligible reaction under these conditions. Gasification efficiency is plotted against residence time for all tested temperatures in Figure 8. A representative Raman spectrum showing reaction products is available in Figure S7.

3.3. Isopropyl Alcohol

Production of H_2 and acetone from IPA begin simultaneously and in nearly equimolar quantities from 4 - 6 s at 560 °C, as shown in Figure 9. Acetone can subsequently decompose to several different product species, which leads to its maximum observed yield of 0.72 mol-C_3H_6O/mol-IPA. To identify acetone decomposition products, SCWG of acetone was performed at 560 °C for 8 s. The collected Raman spectrum is available in Figure S9, from which major acetone gasification products were identified as acetic acid and CH_4, with minor yields of H_2, CO, CO_2, ethylene, and ethane. The formation of acetic acid from IPA at 7 s in Figure 9 supports this observation, as does the minor production of methane in Figure 10. The observed product formation profiles suggest the proposed acetone decomposition pathways presented in

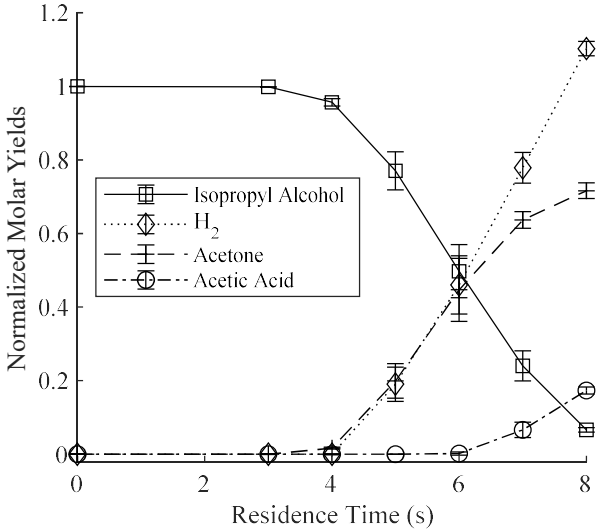

Figure 9: Formation and decomposition of major reaction products during SCWG of IPA at 560 °C

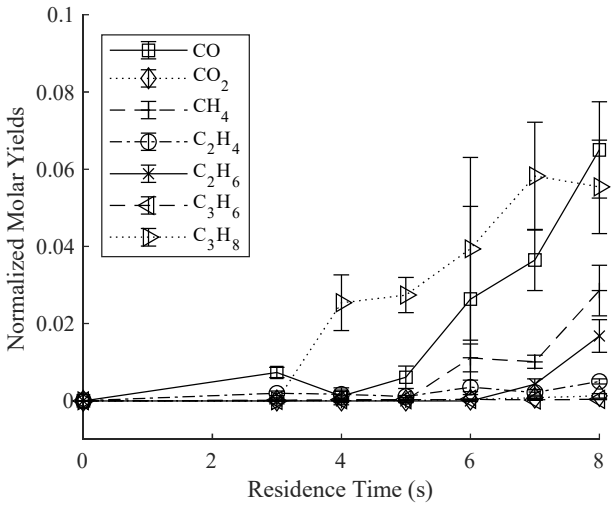

Figure 10: Formation and decomposition of minor reaction products during SCWG of IPA at 560 °C

Figure 11. Analysis of IPA data shows many similarities with trends from SCWG of methanol and ethanol, such as the delayed appearance of CO_2 at 7 s. Only trace amounts of C_2H_4, and C_2H_6 are witnessed, indicating that conversion of acetone to these products is not favorable.

Trace propene yields are detected, which rapidly hydrogenates to a maximum propane yield of 0.06 mol-C_3H_8/mol-IPA at 7 s. Detection of propene and propane confirm the dehydration pathway is active for SCWG of IPA.

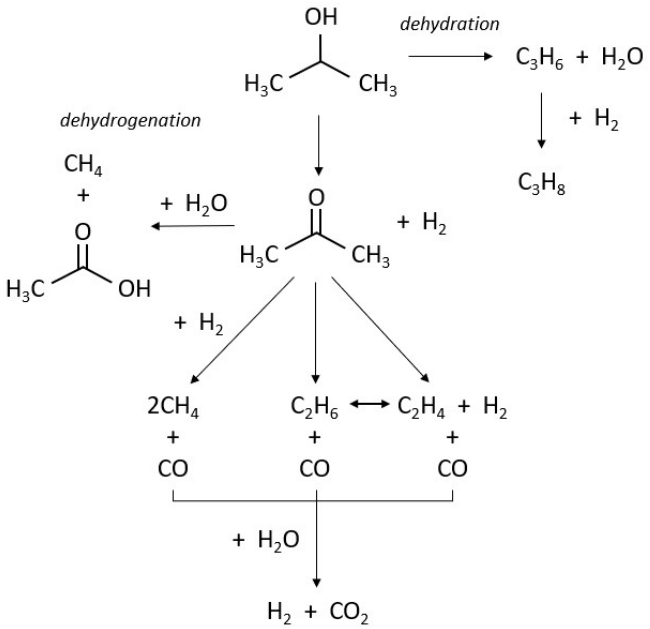

Figure 11: IPA decomposition network in SCW

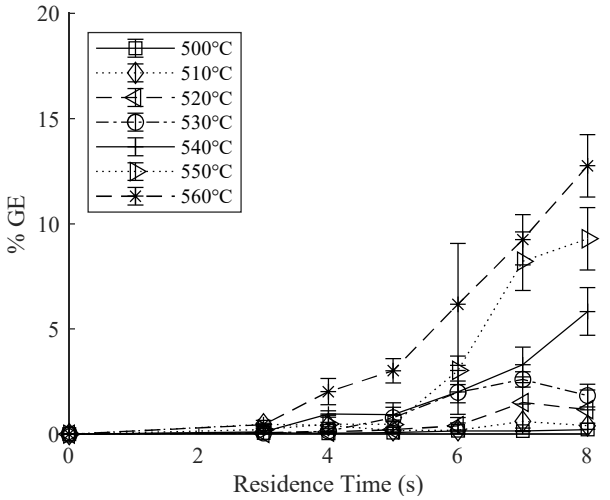

Figure 12: Gasification efficiency of IPA at all tested temperatures

Similar to ethanol, we propose that IPA decomposes via competing dehydrogenation and dehydration reaction pathways, as presented in Figure 11. Many of the reaction pathways are inferred from previous knowledge, such as ethylene hydrogenation and the WGS reaction. Acetic acid is a known refractory SCWG product, thus its decomposition to gaseous products is unlikely to be significant.

Gasification efficiency is plotted against residence time for all tested temperatures in Figure 12. GE is drastically lower for SCWG of IPA than methanol or ethanol, due to the formation of acetone and acetic acid in significant quantities. Decomposition and formation profiles of IPA reaction products at all tested temperatures are available in Figures S4 and S5. A representative Raman spectrum of IPA decomposition products is presented in Figure S8.

4. Discussion

The use of *in situ* Raman spectroscopy allows us to perform experiments with much shorter residence times than most previous studies. From the resulting decomposition profiles, we infer that the primary mechanisms driving the decomposition of alcohols in SCW are chain-branching, free radical reactions. Based on reaction profiles which consistently show a reaction induction time between 3 and 8 s, we conclude that radical pooling is a key step facilitating alcohol decomposition. The importance of free radical reactions to SCWG chemistry is not particularly surprising, but it is important to consider the chain-

branching behavior further, as several previous studies have assumed first-order reaction kinetics for modeling alcohol decomposition in SCW. The next step is to distinguish between reaction initiation steps, propagation steps, and termination steps, considering experimental results presented here and in previously mentioned studies.

Previous modeling and experimental work have shown that oxidation chemistry of alcohols in SCW is closely analogous to oxidation chemistry of alcohols under standard combustion conditions [23]. It follows that reactions of alcohols in SCW without an oxidant would involve similar mechanisms as those already described in the pyrolysis and combustion literature involving homolytic dissociation reactions and non-oxidative radical chain reactions.

4.1. Reaction Initiation Mechanisms

The most probable reaction initiation step during non-catalytic SCWG is homolytic dissociation of the parent alcohol via scission of the weakest bond, namely the C-O (methanol) or the C-C (ethanol and IPA) bond. However, Chakinala et al. [15] reported that alcohols are mostly stable in SCW up to 600 °C in the absence of a catalysts, which is mostly confirmed by the long conversion times reported in other batch studies in this temperature region [7, 17]. Thus, homolytic dissociation is not a likely initiation step during continuous SCWG at 500 to 560 °C. Much more likely is that radicals are initially generated through adsorption and decomposition mechanisms on the catalytic surface of the reactor walls. This adsorption and decomposition step is thought to proceed through adsorption of an H from the parent hydrocarbon onto the catalytic surface, followed by release of the remainder of the parent molecule back into the bulk flow in the form of a highly-reactive free radical [10, 24].

If homolytic dissociation of ethanol or IPA were key initiation steps, this would initially generate methyl radicals in the bulk flow through C-C bond scission, leading to yields of CH_4 and ethane prior to observable yields of ethylene, acetaldehyde, or acetone. However, this is not the behavior observed in these experiments. For SCWG of ethanol, methane is only observed after significant formation of acetaldehyde.

As further evidence for this hypothesis, alcohol combustion studies have shown that homolytic dissociation of methanol to methyl (CH_3) and hydroxyl (OH) radicals through C-O bond cleavage is a negligible reaction mechanism [25, 26]. The absence of CH_4 and ethane as products from methanol SCWG indicates that this finding holds in SCW environments, as both would be present as reaction products if methyl radicals were formed in the reaction environment. It follows that C-O bond cleavage during SCWG of ethanol and IPA would also be negligible.

4.2. Reaction Propagation Mechanisms

Once intermediate radicals are catalytically generated, they can initiate chain reactions through propagation steps, such as H abstraction from the parent alcohol via intermediate radicals. For methanol, initial catalytic H abstraction most probably forms CH_2OH radicals. A less probable step is also available, via O-H scission to CH_3O. Both of these steps are consistent with the mechanism proposed by Chakinala et al. [12]. Each radical rapidly reaches formaldehyde through an additional H abstraction step, generating a growing radical pool and propagating the chain-branching reaction. Formaldehyde rapidly reacts to CO and H_2; aldehydes are highly sensitive to radical attack and are short-lived at the conditions tested [26].

In the case of ethanol, Norton and Dryer [26] concluded that the variation in observed products during ethanol oxidation was largely dependent on the initial site of H abstraction. This finding seems to hold for SCWG of ethanol. Three potential C_2H_5O isomers are energetically available based on relative bond energies: CH_3CHOH, C_2H_4OH, and CH_3CH_2O [26, 27]. These isomers can then react via the following dissociation reactions:

$$CH_3CHOH \rightarrow C_2H_4O + H$$

$$C_2H_4OH \rightarrow C_2H_4 + OH$$

$$CH_3CH_2O \rightarrow CH_2O + CH_3$$

all of which produce more free radicals in the reaction environment to speed the initial H abstraction step. No formaldehyde was detected during SCWG of ethanol; it is likely that it decomposes to CO and H_2 too quickly to be detected.

It is reasonable to extrapolate dominant IPA mechanisms based on methanol and ethanol mechanisms. The C_3 chain affords four potential C_3H_7O isomers after H abstraction from the parent IPA molecule. If the reaction behavior is similar to ethanol, (and the similarity of the reaction network and decomposition profiles seems to indicate that it is), these isomers could plausibly react via the following reactions:

$$CH_3CH_2CHOH \rightarrow C_3H_6O + H$$

$$CH_3CHCH_2OH \rightarrow C_3H_6O + H$$

$$C_3H_6OH \rightarrow C_3H_6 + OH$$

$$CH_3CH_2CH_2O \rightarrow CH_2O + C_2H_5$$

Acetone is the dominant intermediate from IPA decomposition. Similar to formaldehyde and acetaldehyde, the C=O double bond in the acetone molecule is stable under SCWG conditions. Acetone decomposition in SCW must proceed through C-C bond scission, forming a methyl radical and a methylcarbonyl radical (C_2H_3O). The methylcarbonyl radical can hydrolyze to form acetic acid and an H radical, which appears to be the favored acetone reaction pathway. The presence of methyl radicals can explain the major yield of CH_4 from SCWG of acetone, and the minor yields of ethane and ethylene. Because the molar yields of acetic acid are consistently higher than the molar yield of CH_4, it seems highly unlikely that acetone can simultaneously lose both methyl radicals along the hydrogenation pathway in Figure 9; however, it is included for completeness.

4.3. Reaction Termination Mechanisms

Stable end-products during the SCWG of all alcohols studied include H_2, CO_2, CH_4, ethane, and propane. H_2 is produced through the coupling of two H radicals, either in the bulk flow or through abstraction of a H atom via a H radical. CO_2 is reached through the forward WGS reaction, which is favored over the reverse reaction under high-temperature, aqueous conditions. Methyl radicals (likely only formed from acetaldehyde or acetone) are quick to abstract H from other

hydrocarbons to form stable CH_4, or can combine to form ethane, although this is much less probable.

5. Conclusions

Primary alcohols are gasified in SCW at temperatures between 500 and 560 °C for residence times between 3 and 8 s. *In situ* Raman spectroscopy facilitates rapid data collection at short residence times. Data collected at short residence times demonstrate the procession of chain-branching, free radical mechanisms for all primary alcohols. Clearly, alcohol decomposition in SCW does not follow first-order reaction behavior at these conditions. H abstraction is a key mechanism for all three alcohols studied, confirmed by the dominance of dehydrogenation pathways to formaldehyde, acetaldehyde, and acetone. Based on the work of DiLeo and Savage [7], along with comparison of these results to studies performed in batch reactors [12, 17], we also propose initial H abstraction mechanisms are facilitated by the presence of catalytic reactor walls. Radical pooling likely leads to further H abstraction, which is analogous to known alcohol pyrolysis mechanisms and could explain high char yields witnessed during SCWG of aromatic compounds. A more complete understanding of SCWG reaction mechanisms allows for prediction of decomposition pathways of more complex organic compounds.

Acknowledgements

Funding for this work was provided by the Defense Threat Reduction Agency (DTRA) – Grant HDTRA1-17-1-0001. Special thanks to Vedant Maheshwari and Anmol Purohit for assistance collecting experimental data, and to David Gorman and Kartik Tiwari for help with the initial design and fabrication of the reactor used for these experiments.

References

[1] A. Kruse, Supercritical water gasification, Biofuels Bioprod. Biorefin. 2 (2008) 415-437. https://doi.org/10.1002/bbb.93.

[2] P.E. Savage, Organic chemical reactions in supercritical water, Chem. Rev. 99 (1999) 603-622. https://doi.org/10.1021/cr9700989.

[3] Y. Guo, S.Z. Wang, D.H. Xu, Y.M. Gong, H.H. Ma, X.Y. Tang, Review of catalytic supercritical water gasification for hydrogen production from biomass, Ren. Sust. Energy Rev. 14 (2010) 334-343. https://doi.org/10.1016/j.rser.2009.08.012.

[4] M.J. Antal Jr., S.G. Allen, D. Schulman, X. Xu, R.J. Divilio, Biomass Gasification in Supercritical Water, Ind. Eng. Chem. Res. 39 (2000) 4040-4053. https://doi.org/10.1021/ie0003436.

[5] A.H. Zacher, M.V. Olarte, D.M. Santosa, D.C. Elliott, S.B. Jones, A review and perspective of recent bio-oil hydrotreating research, Green Chemistry 16 (2014) 491-515. https://doi.org/10.1039/C3GC41382A

[6] J. Scherzer, A.J. Gruia, Hydrocracking Science and Technology, Taylor & Francis, Abingdon, 1996.

[7] G.J. DiLeo, P.E. Savage, Catalysis during methanol gasification in supercritical water, J. Supercrit. Fluids 39 (2006) 228-232. https://doi.org/10.1016/j.supflu.2006.01.004.

[8] B.R. Pinkard, D.J. Gorman, K. Tiwari, J.C. Kramlich, P.G. Reinhall, I.V. Novosselov, Review of gasification of organic compounds in continuous-flow, supercritical water reactors, Ind. Eng. Chem. Res. 57 (2018) 3471-3481. https://doi.org/10.1021/acs.iecr.8b00068.

[9] B.R. Pinkard, D.J. Gorman, K. Tiwari, E.G. Rasmussen, J.C. Kramlich, P.G. Reinhall, I.V. Novosselov, Supercritical water gasification: practical design strategies and operational challenges for lab-scale, continuous flow reactors, Heliyon 5 (2019) e01269. https://doi.org/10.1016/j.heliyon.2019.e01269.

[10] B.R. Pinkard, D.J. Gorman, E.G. Rasmussen, J.C. Kramlich, P.G. Reinhall, I.V. Novosselov, Kinetics of formic acid decomposition in subcritical and supercritical water - a Raman spectroscopic study, Int. J. Hydrog. Energy 44 (2019) 31745-31756. https://doi.org/10.1016/j.ijhydene.2019.10.070.

[11] K. Tiwari, B.R. Pinkard, D.J. Gorman, J. Davis, J.C. Kramlich, P.G. Reinhall, I.V. Novosselov, Computational modeling of mixing and gasification in continuous-flow supercritical water reactor, Proceedings of the 12th International Symposium on Supercritical Fluids (2018).

[12] A.G. Chakinala, S. Kumar, A. Kruse, S.R.A. Kersten, W.P.M. van Swaaij, D.W.F. Brilman, Supercritical water gasification of organic acids and alcohols: The effect of chain length, J. Supercrit. Fluids 74 (2013) 8-21. https://doi.org/10.1016/j.supflu.2012.11.013.

[13] N. Boukis, V. Diem, W. Habicht, E. Dinjus, Methanol reforming in supercritical water, Ind. Eng. Chem. Res. 42 (2003) 728-735. https://doi.org/10.1021/ie020557i.

[14] J.G. van Bennekom, R.H. Venderbosch, D. Assink, H.J. Heeres, Reforming of methanol and glycerol in supercritical water, J. Supercrit. Fluids 58 (2011) 99-113. https://doi.org/10.1016/j.supflu.2011.05.005.

[15] K. Yoshida, C. Wakai, N. Matubayasi, M. Nakahara, NMR spectroscopic evidence for an intermediate of formic acid in the water-gas-shift reaction, J. Phys. Chem. A 108 (2004) 7479-7482. https://doi.org/10.1021/jp047086t.

[16] J. Schanzenbächer, J.D. Taylor, J.W. Tester, Ethanol oxidation and hydrolysis rates in supercritical water, J. Supercrit. Fluids 22 (2002) 139-147. https://doi.org/10.1016/S0896-8446(01)00119-X.

[17] T. Arita, K. Nakahara, K. Nagami, O. Kajimoto, Hydrogen generation from ethanol in supercritical water without catalyst, Tetrahedron Lett. 48 (2003) 1083-1086. https://doi.org/10.1016/S0040-4039(02)02704-1.

[18] M.J. Antal Jr., M. Carlsson, X. Xu, Mechanism and kinetics of the acid-catalyzed dehydration of 1- and 2-propanol in hot compressed liquid water, Ind. Eng. Chem. Res. 37 (1998) 3820-3829. https://doi.org/10.1021/ie980204c.

[19] B.R. Pinkard, D.J. Gorman, V. Maheshwari, J.C. Kramlich, P.G. Reinhall, I.V. Novosselov, Raman spectroscopic data from formic acid decomposition in subcritical and supercritical water, Data Brief, (2019) Under Review.

[20] E. Kriesten, F. Alsmeyer, A. Bardow, W. Marquardt, Fully automated indirect hard modeling of mixture spectra, Chemom. Intell. Lab. Syst. 91 (2008) 181-193. https://doi.org/10.1016/j.chemolab.2007.11.004.

[21] F. Alsmeyer, H.J. Koß, W. Marquardt, Indirect spectral hard modeling for the analysis of reactive and interacting mixtures, Appl. Spectrosc. 58 (2004) 975-985.

[22] P. Beumers, T. Brands, H.J. Koss, A. Bardow, Model-free calibration of Raman measurements of reactive systems: Application to monoethanolamine/water/CO_2, Fluid Phase Equilib. 424 (2016) 52-57. https://doi.org/10.1016/j.fluid.2015.10.004.

[23] S.F. Rice, E Croiset, Oxidation of simple alcohols in supercritical water III. Formation of intermediates from ethanol, Ind. Eng. Chem. Res. 40 (2001) 86-93. https://doi.org/10.1021/ie000372g.

[24] J. Wei, E. Iglesia, Isotopic and kinetic assessment of the mechanism of reactions of CH_4 with CO_2 or H_2O to form synthesis gas and carbon on nickel catalysts, J. Catal. 224 (2004) 370-383. https://doi.org/10.1016/j.jcat.2004.02.032.

[25] T.J. Held, F.L. Dryer, A comprehensive mechanism for methanol oxidation, Int. J. Chem. Kin. 30 (1998) 805-830. https://doi.org/10.1002/(SICI)1097-4601(1998)30:11<805::AID-KIN4>3.0.CO;2-Z.

[26] T.S. Norton, F.L. Dryer, An experimental and modeling study of ethanol oxidation kinetics in an atmospheric pressure flow reactor, Int. J. Chem. Kin. 24 (1992) 319-344. https://doi.org/10.1002/kin.550240403.

[27] N.M. Marinov, A detailed chemical kinetic model for high temperature ethanol oxidation, Int. J. Chem. Kin. 31 (1999) 183-220. https://doi.org/10.1002/(SICI)1097-4601(1999)31:3<183::AID-KIN3>3.0.CO;2-X.

[28] G. Magnotti, U. KC, P.L. Varghese, R.S. Barlow, Raman spectra of methane, ethylene, ethane, dimethyl ether, formaldehyde and propane for combustion applications, J. Quant. Spectrosc. Radiat. Transf. 163 (2015) 80-101. https://doi.org/10.1016/j.jqsrt.2015.04.018.